

Vacuum stability at cryogenic temperature

WP4 - Activity at LNF

Amsterdam, 12/04/2018

Luisa Spallino

Marco Angelucci

Roberto Cimino



In March, during EuroCirCol Meeting in Frascati

Thermal desorption measurements: preliminary results

Desorption processes of Ar from clean Cu and Laser Treated (LASE)-Cu



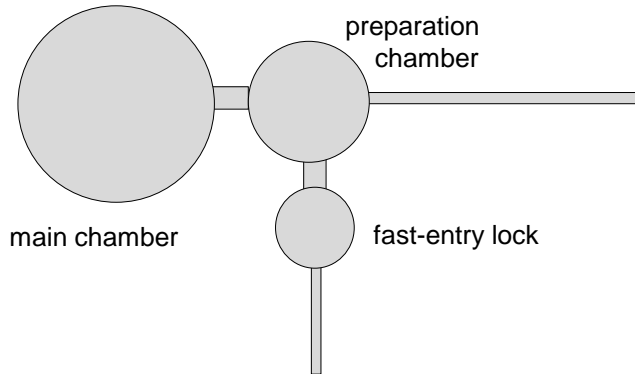
Today, during the EuroCirCol Meeting in Amsterdam

➤ Summary of the main activities

- Dose calibration
- Temperature calibration
- Desorption calibration

➤ Thermal desorption measurements: data analysis

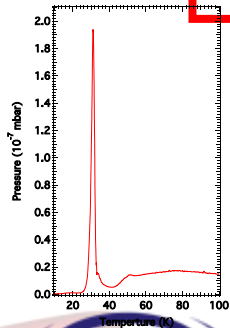
Ultra high vacuum systems



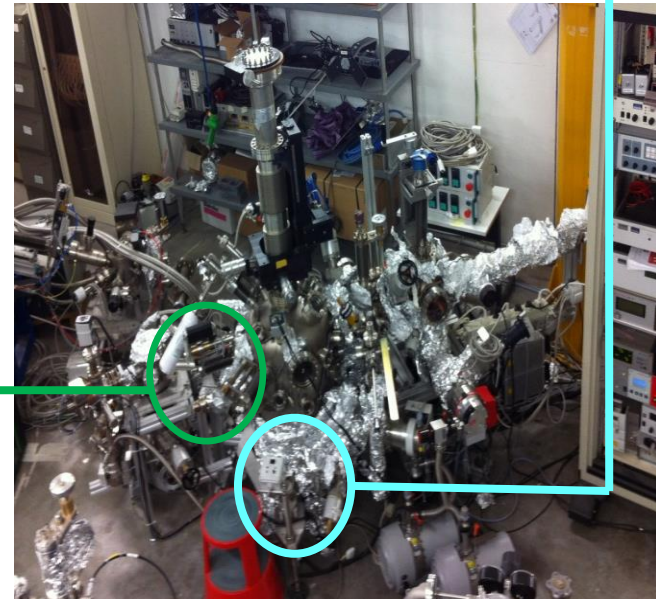
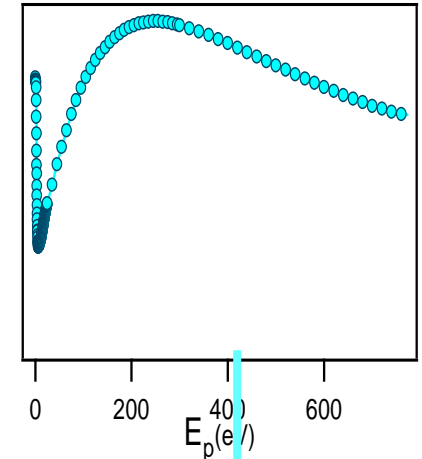
- LNF-cryogenic manipulator
- Sample at 15-300 K

Temperature Programmed Desorption (**TPD**) measurements

Equipment : QMS (Hiden HAL 101 Pic)

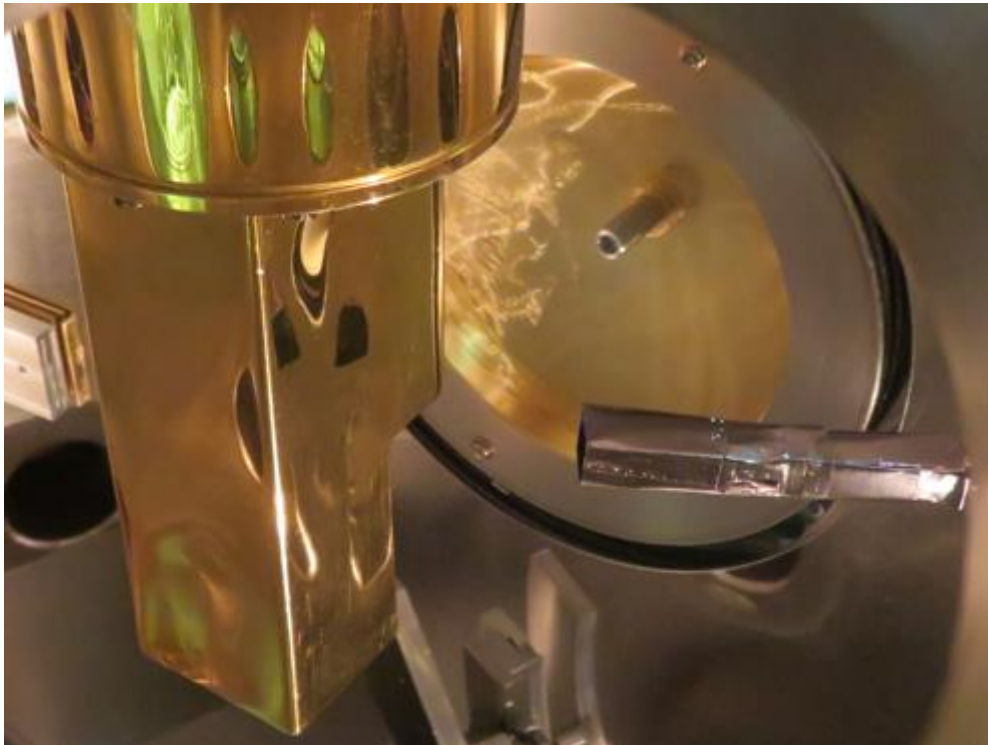


Secondary Electron Yield (**SEY**) measurements
Equipment : Electron gun, Faraday cup

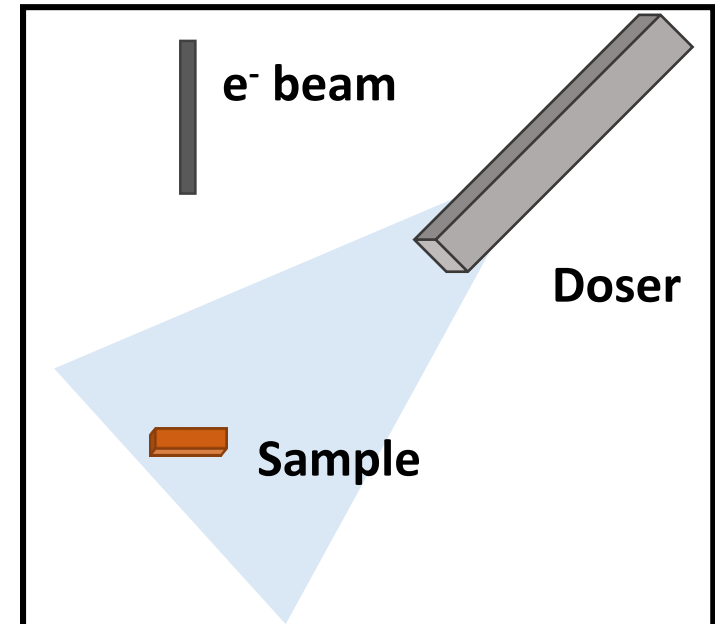


Dose calibration

Gas dosing OLD set-up

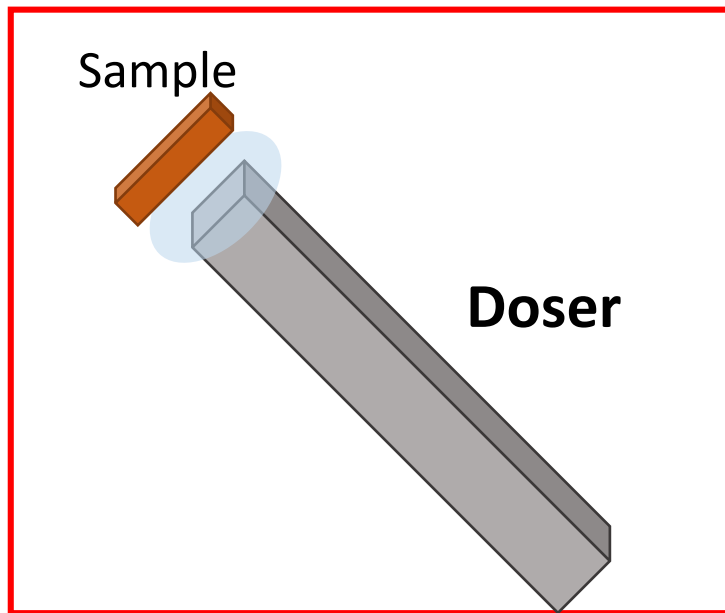


Far from the sample



Gas dosing NEW set-up

Near to the sample

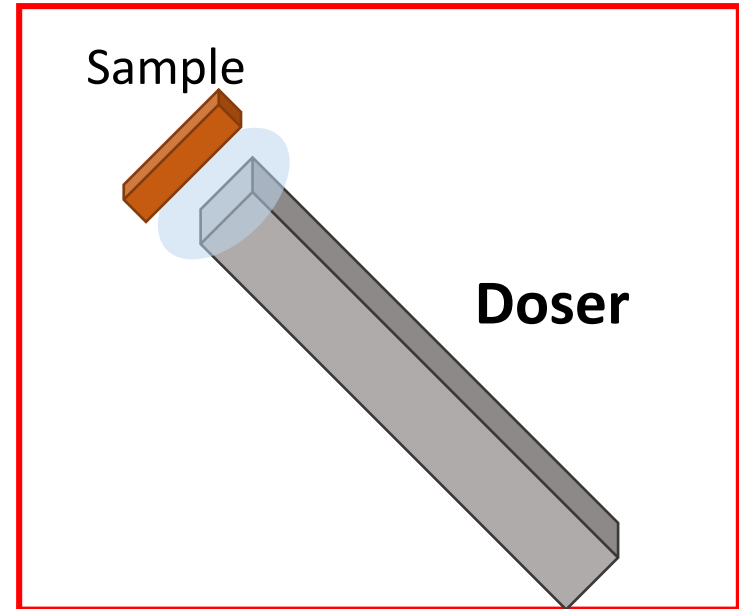
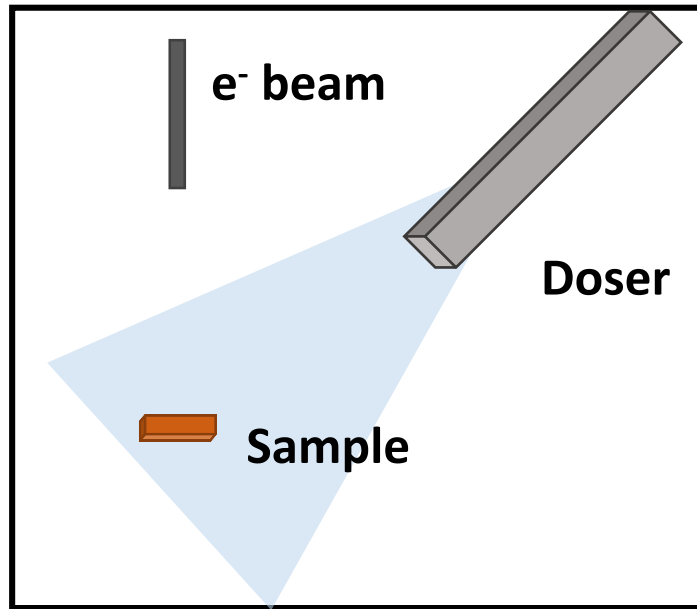


Different local pressure on the sample

1s@ 1.33×10^{-6} mbar corresponds to

Far from the sample

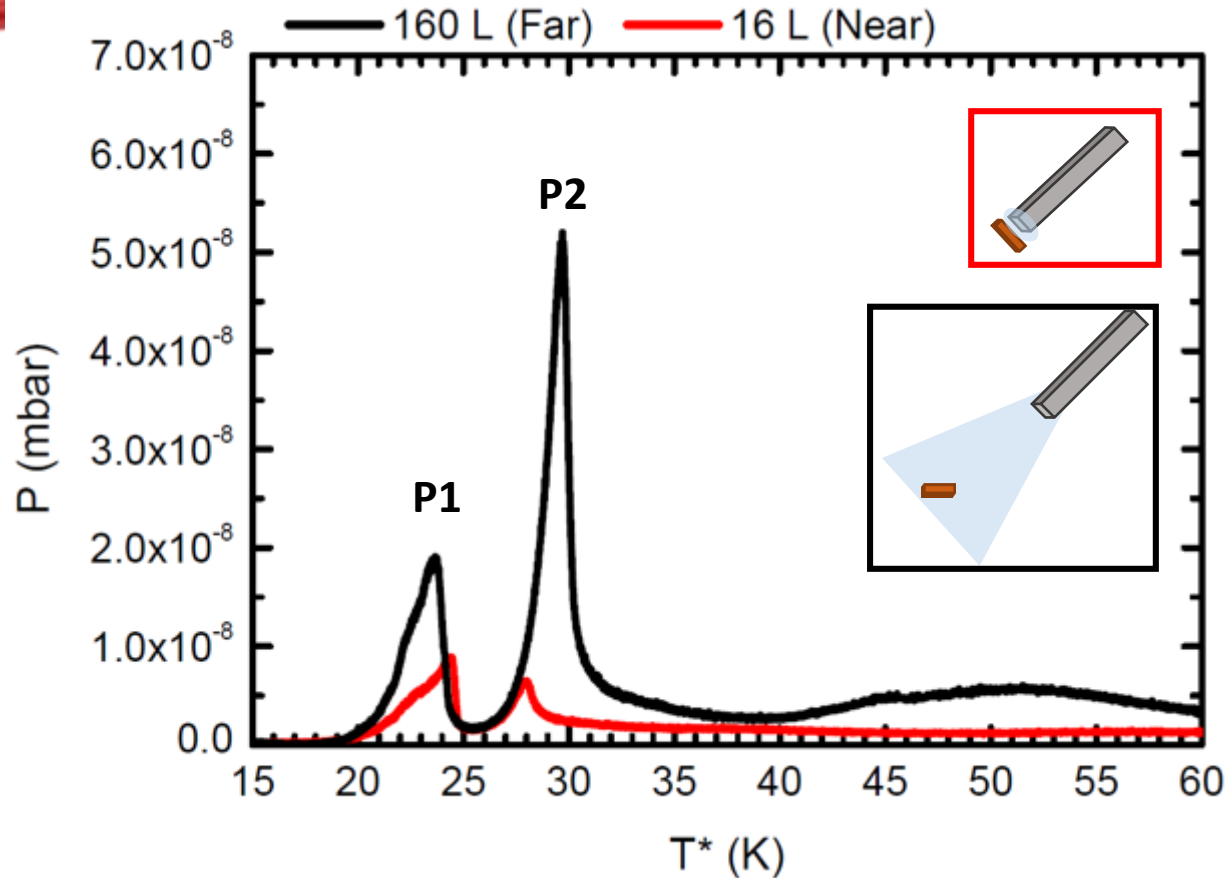
Near to the sample



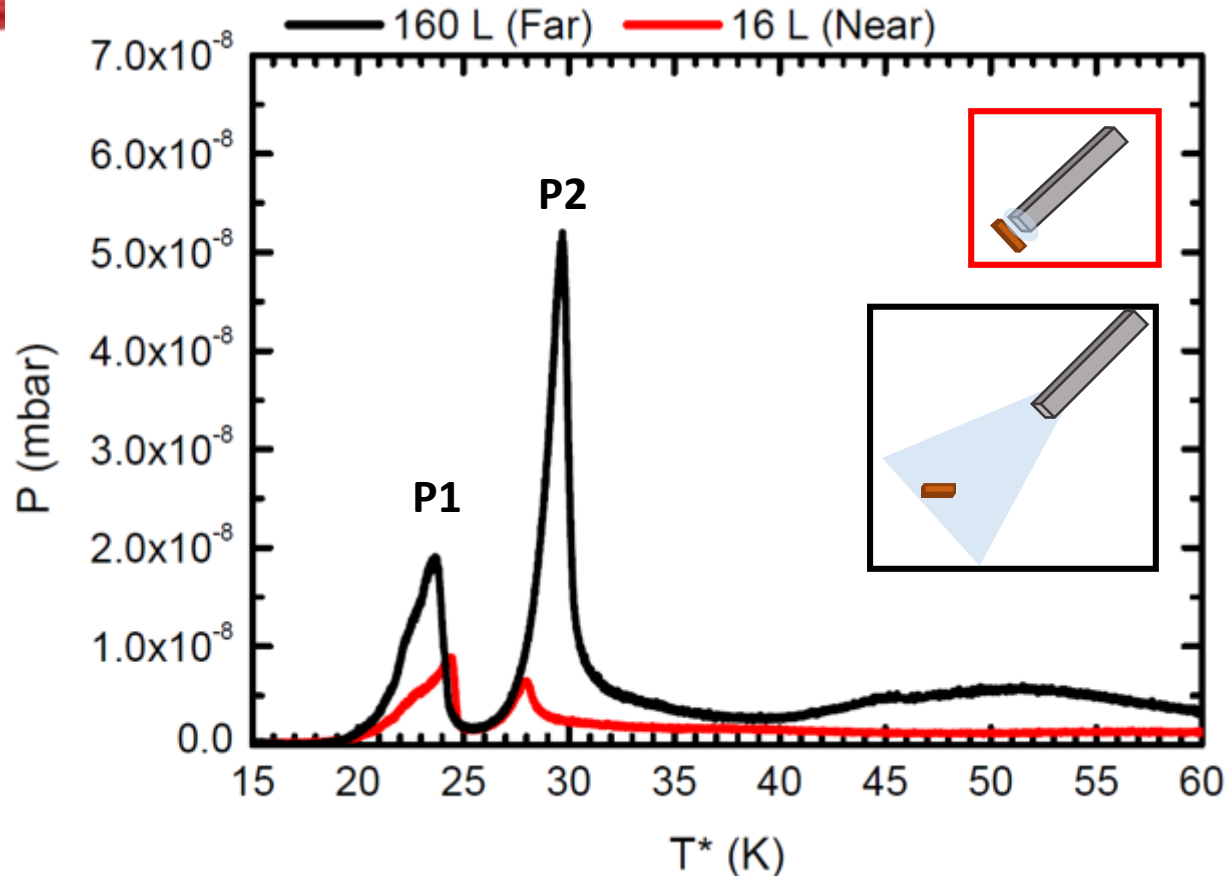
1 Langmuir

≈ 8 Langmuir

Accurate Calibration in progress



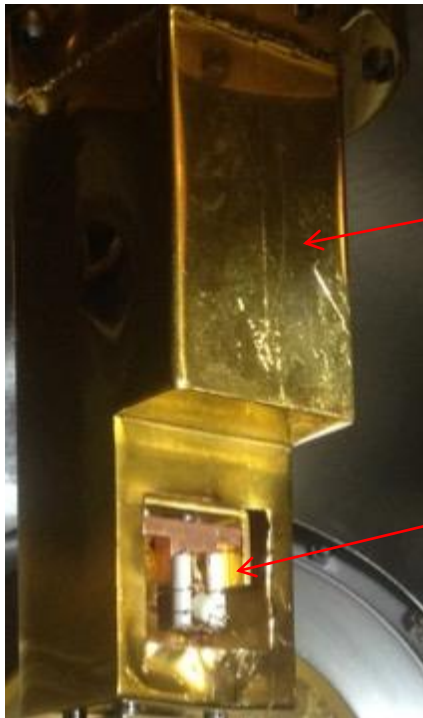
Accurate
Calibration in
progress



Accurate
Calibration in
progress

✓ Putting the doser near the sample is effective for the reduction of the desorption related to the manipulator

LNF-Cryogenic Manipulator

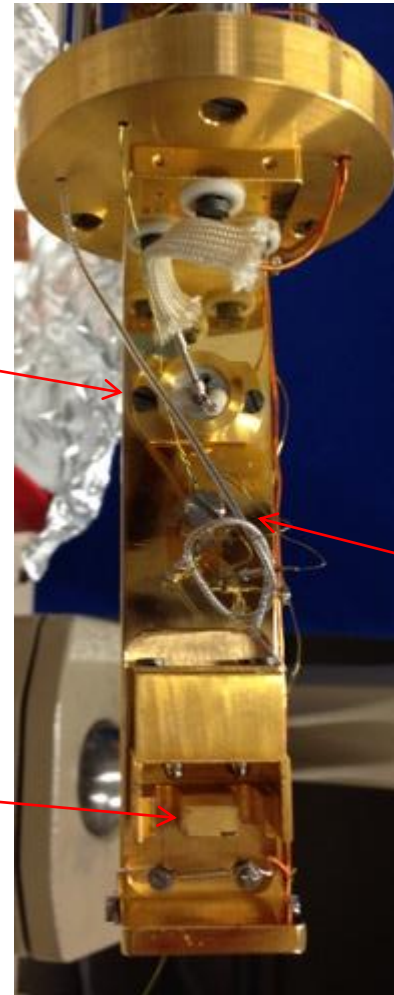


Screen

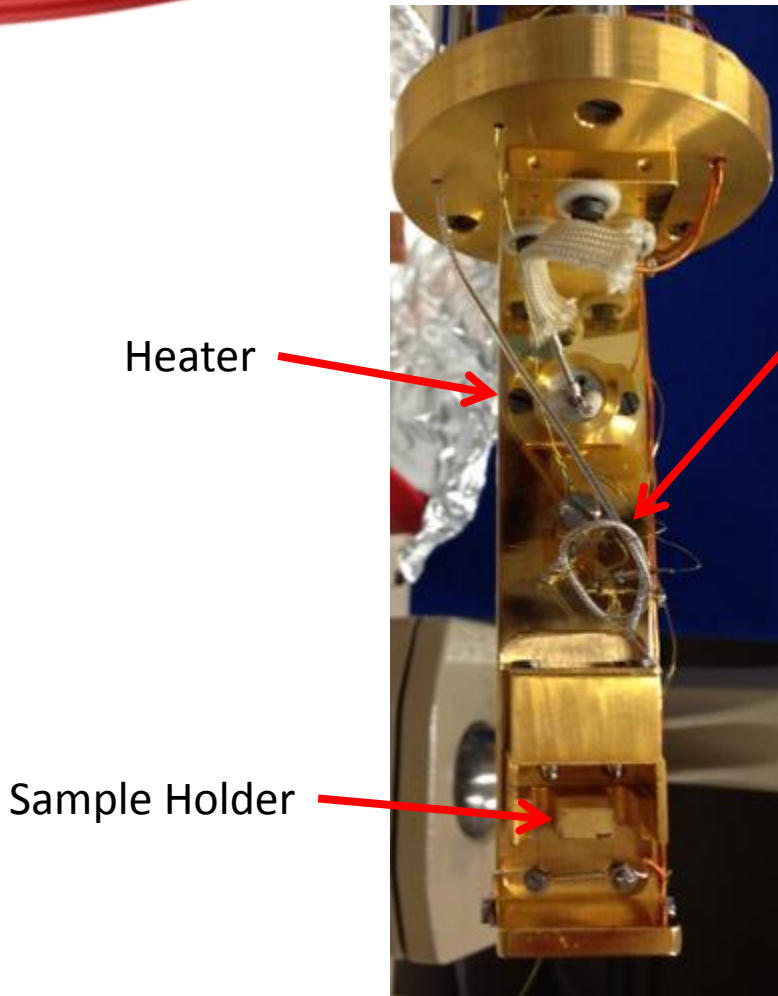
Sample

Heater

Sample Holder

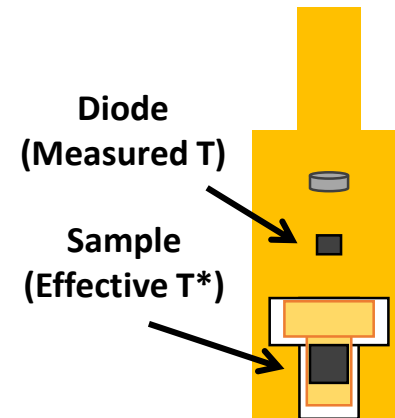


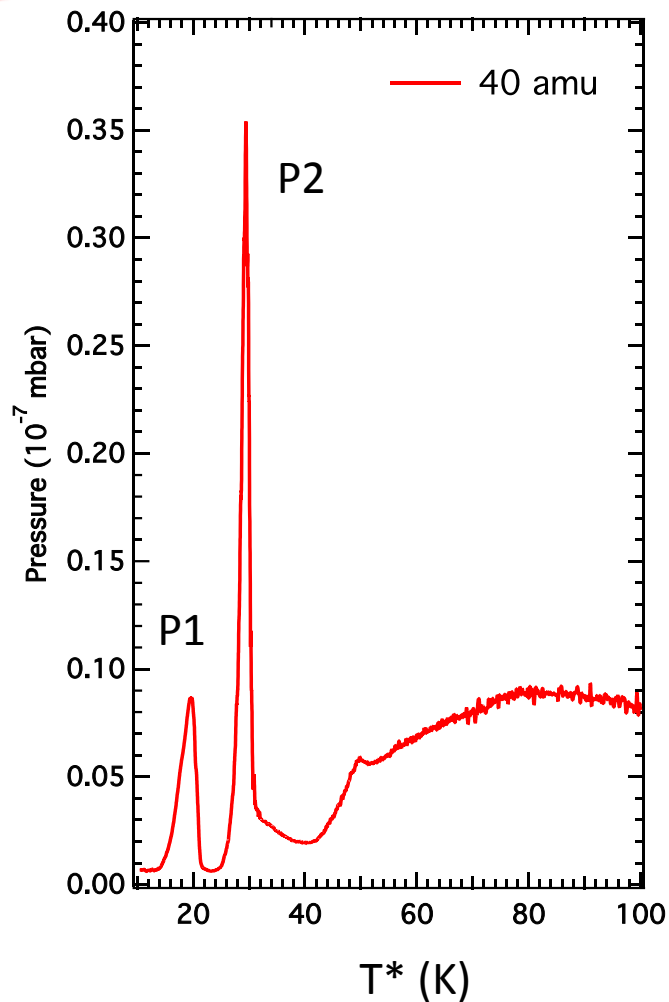
Measured
Temperature



**Measured
Temperature**

Measured Temperature (T^*)
 \neq
Sample Real Temperature (T)





Ar Temperature Programmed Desorption

The **different desorption peaks**
are experimental artefact

clean Ni(111) surface chemisorbed benzene physisorbed benzene

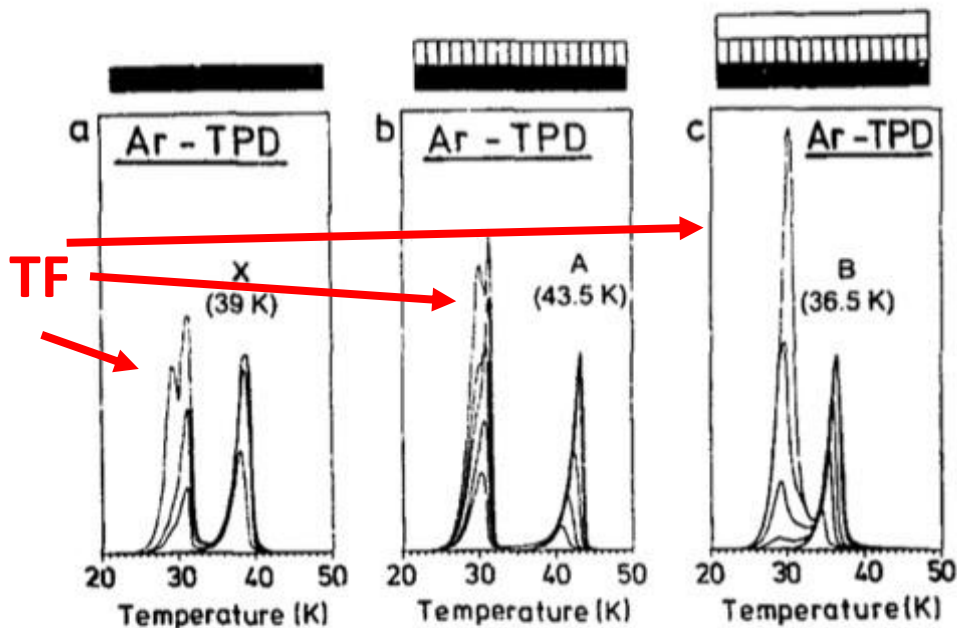


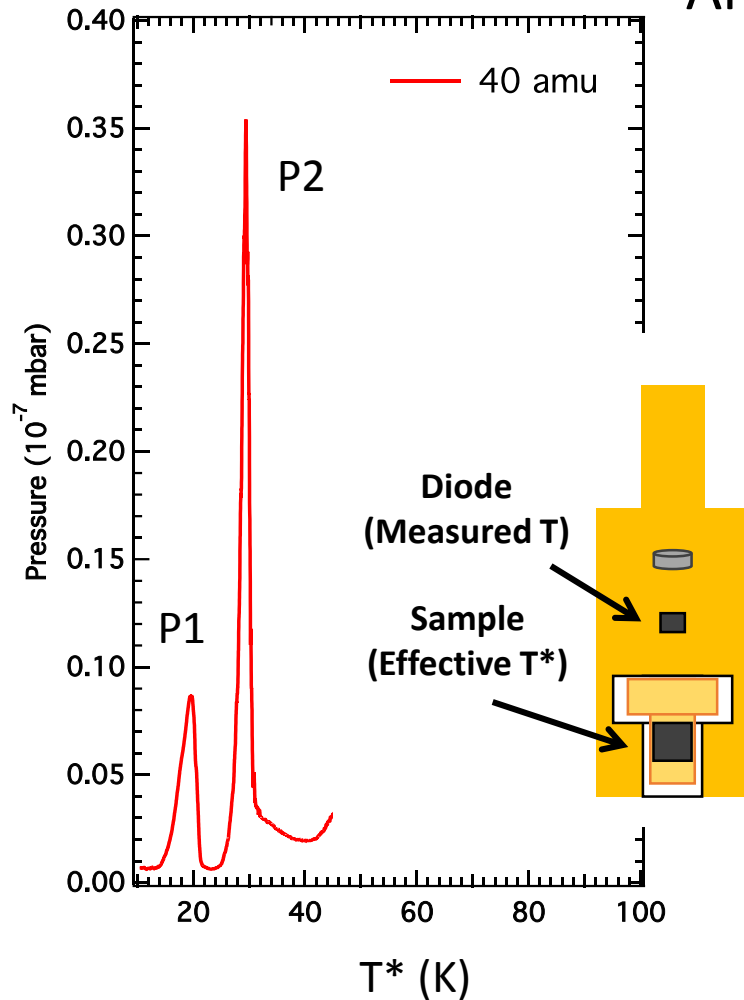
Fig. 1. Argon desorption spectra for increasing argon exposures onto various underlying "substrates": (a) clean Ni(111); (b) saturated chemisorbed $(\sqrt{7} \times \sqrt{7})R19.1^\circ$ benzene layer on Ni(111); (c) saturated first physisorbed benzene layer on top of the chemisorbed layer. Adsorption temperature 22 K; heating rate 1 K/s. The "substrates" are schematically indicated above the corresponding TPD spectra.

Same Desorption temperature of Argon Thick Film (TF) on different substrates

Ar TF desorbs at a unique $T \sim 30$ K

M. Stichler et al.; Surface Science 348 (1996) 370-378

Ar Temperature Programmed Desorption

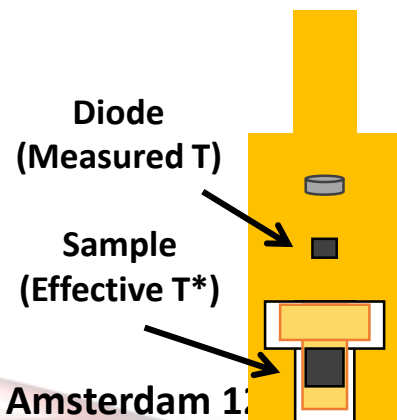
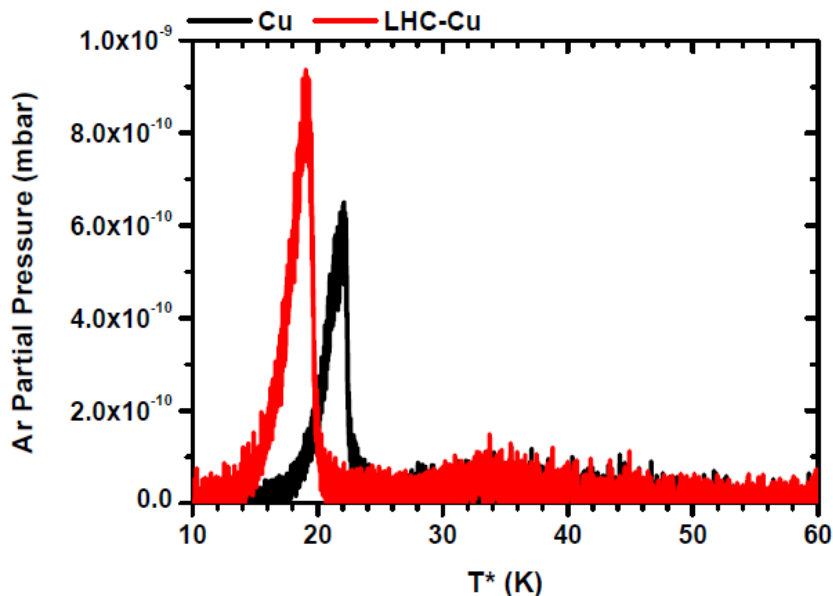


Peak 1: Desorption from sample (“hotter part” at T^*)

Peak 2: Desorption from Manipulator (at T)

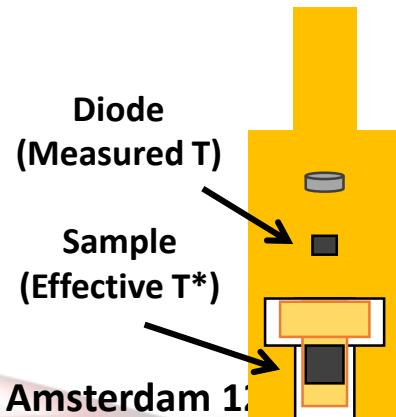
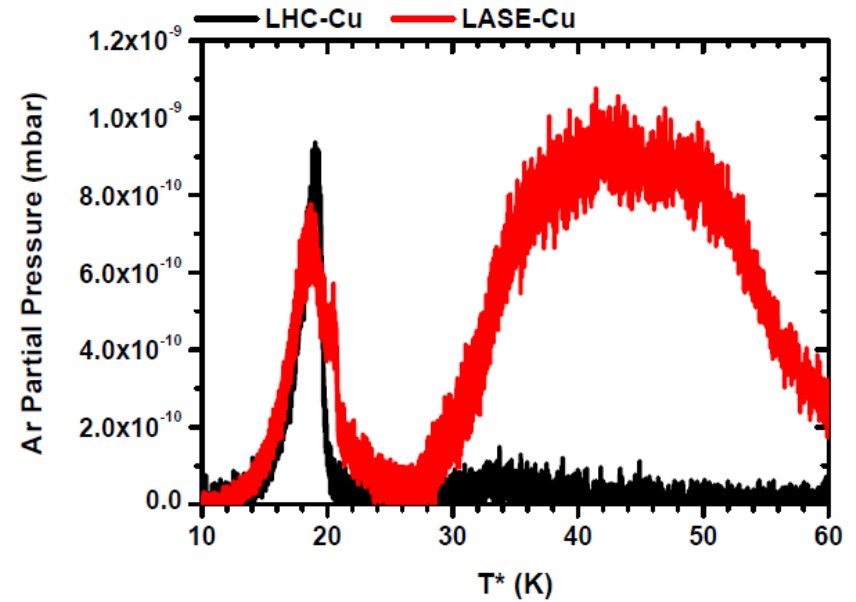
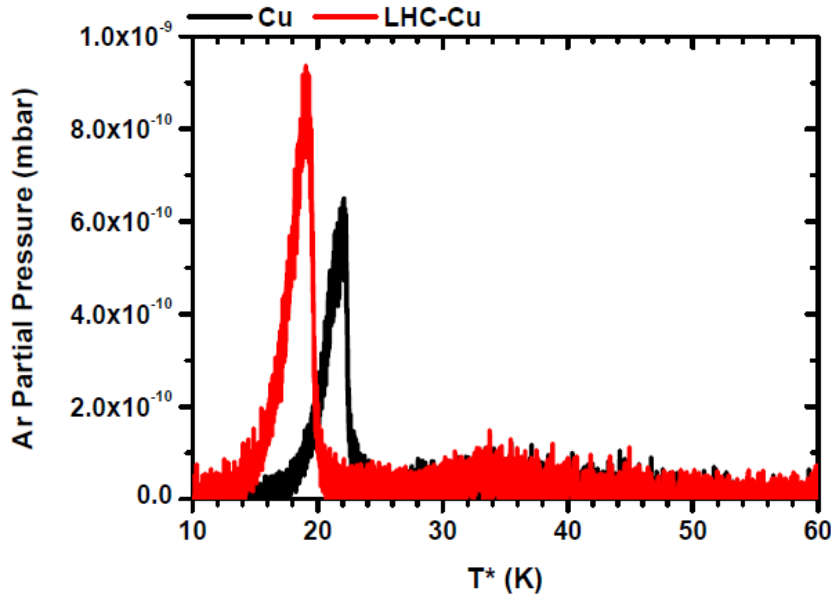
The different desorption peaks are experimental artefact, not real...but **advantageous for us!!!**

T* shift



The effective temperature of LCH sample is higher due to stainless steel core, so its desorption peak appears at a lower T^* respect to Cu!

T* shift



The effective temperature of LCH sample is higher due to stainless steel core, so its desorption peak appears at a lower T^* respect to Cu!

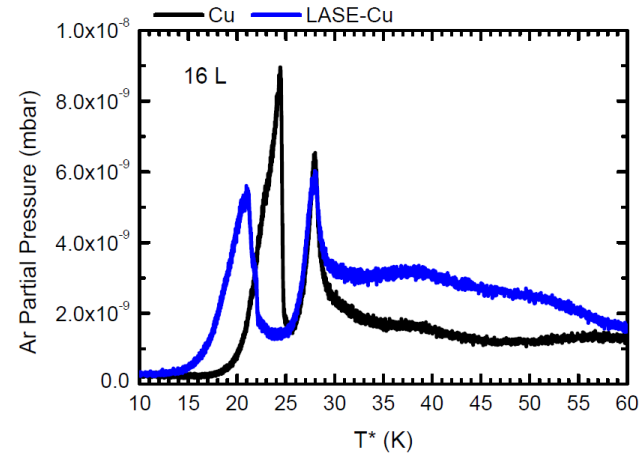
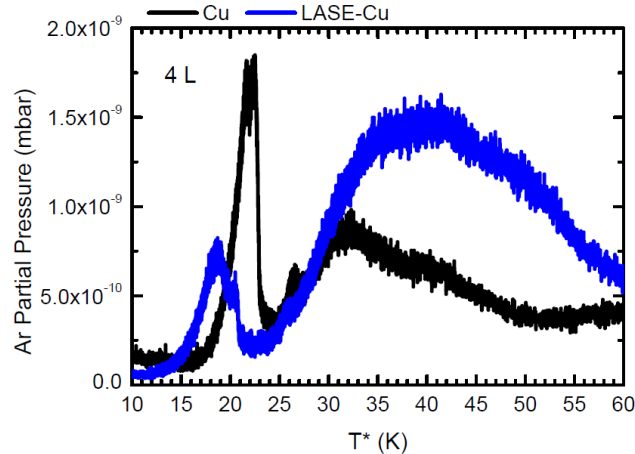
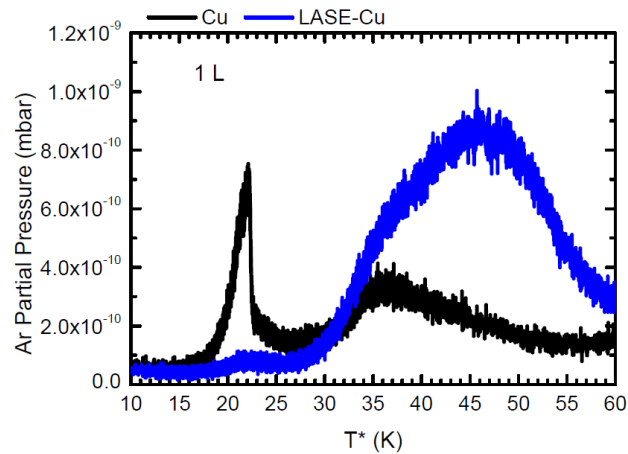


In March, during EuroCirCol Meeting in Frascati

Thermal desorption measurements: preliminary results

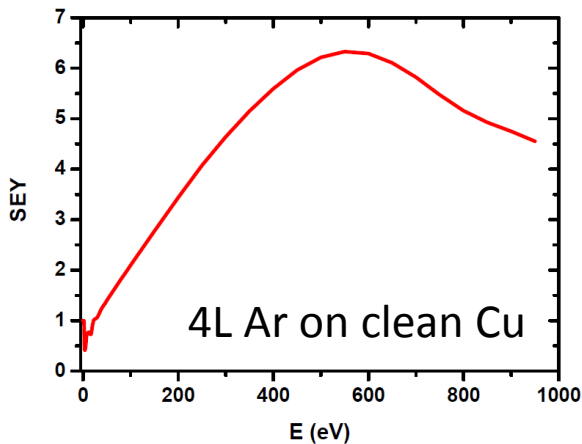
Desorption processes of Ar from clean Cu and Laser Treated (LASE)-Cu

Synopsys of the raw data

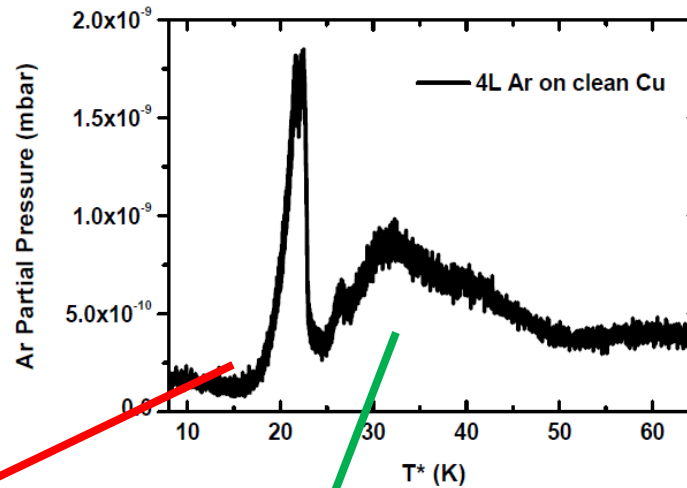


SEY vs T as cross-check for interpreting the thermal desorption curves

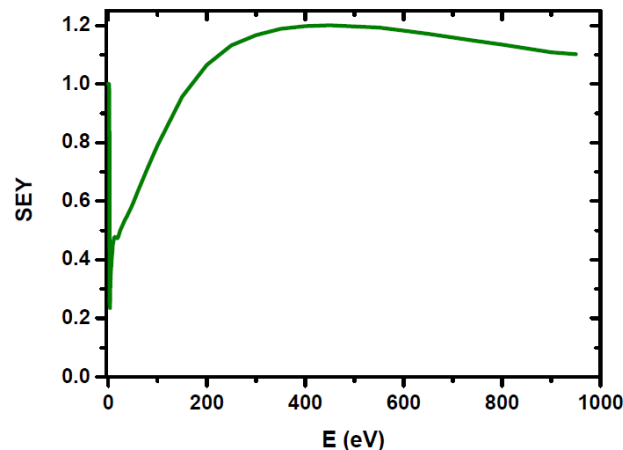
Below T=20 K

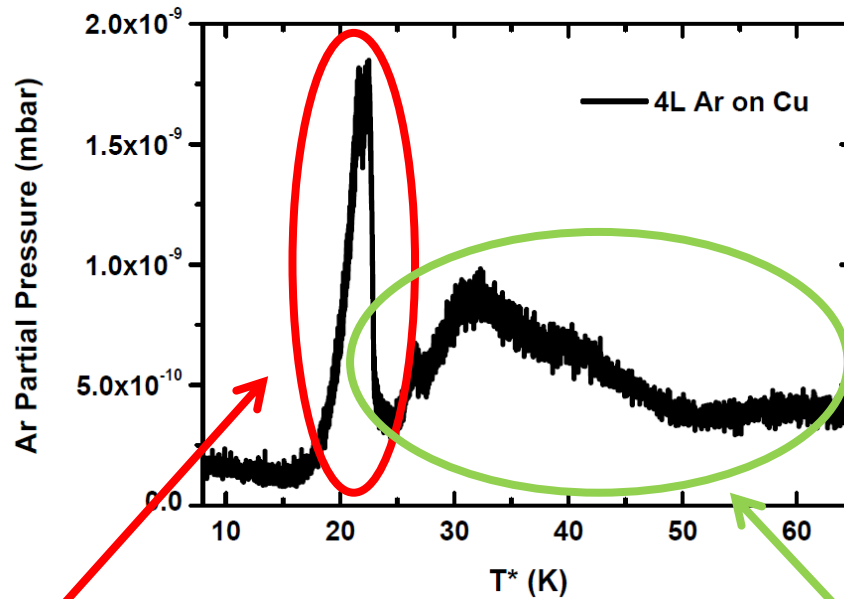


Typical SEY of 1, 4, 16 L of Ar thick film on clean Cu



Above T=30 K

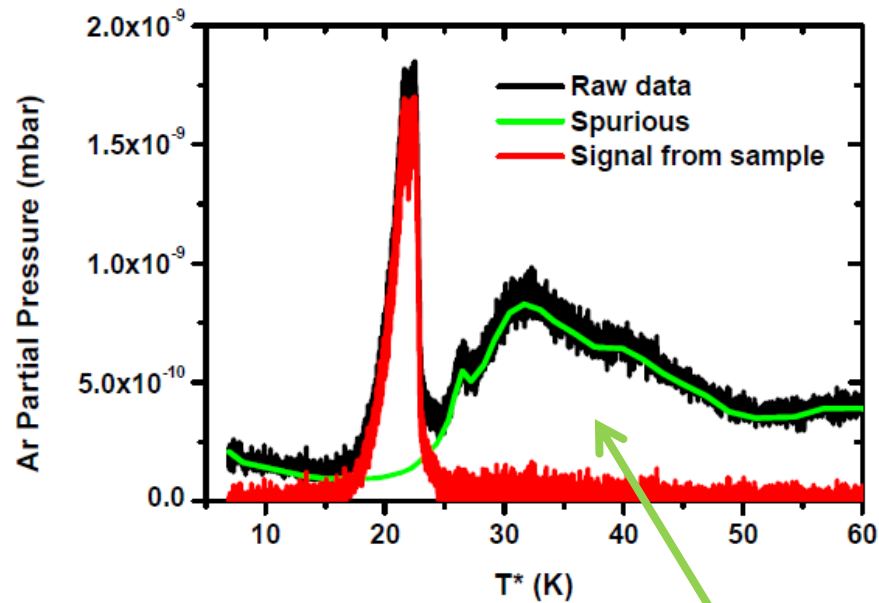




Ar desorption from other part of the system

Ar desorption from sample

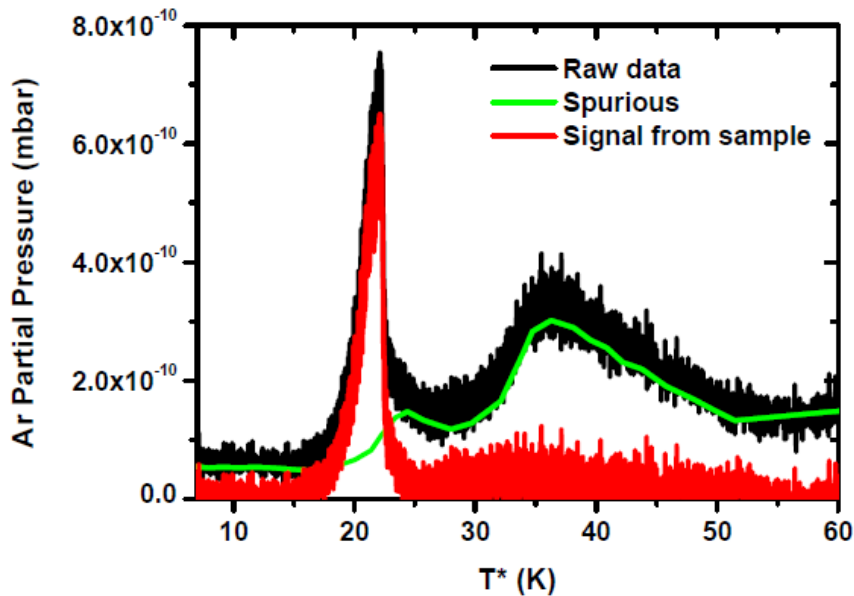
Subtraction of the contribution accounting for the desorption from other part of the system



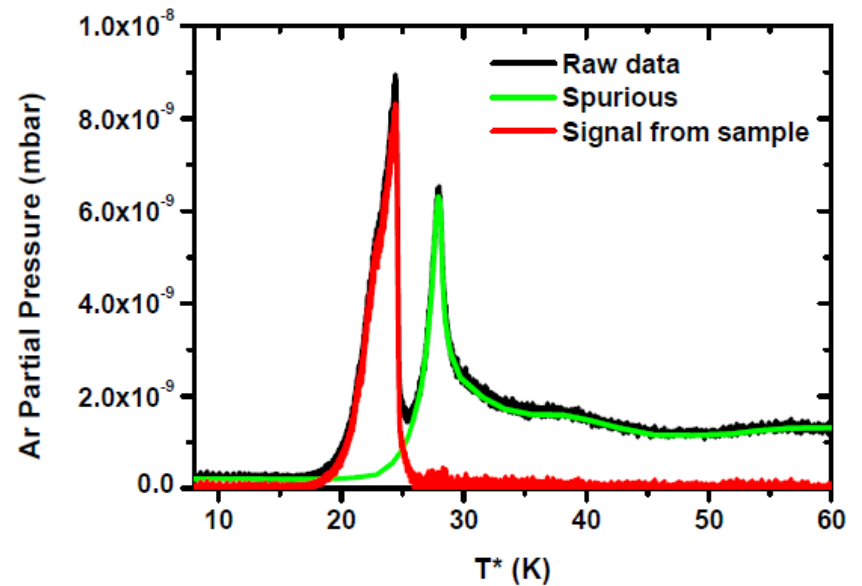
4 L on clean Cu

**Spurious contribution is independent from the sample!!!
It depends on the dose only.**

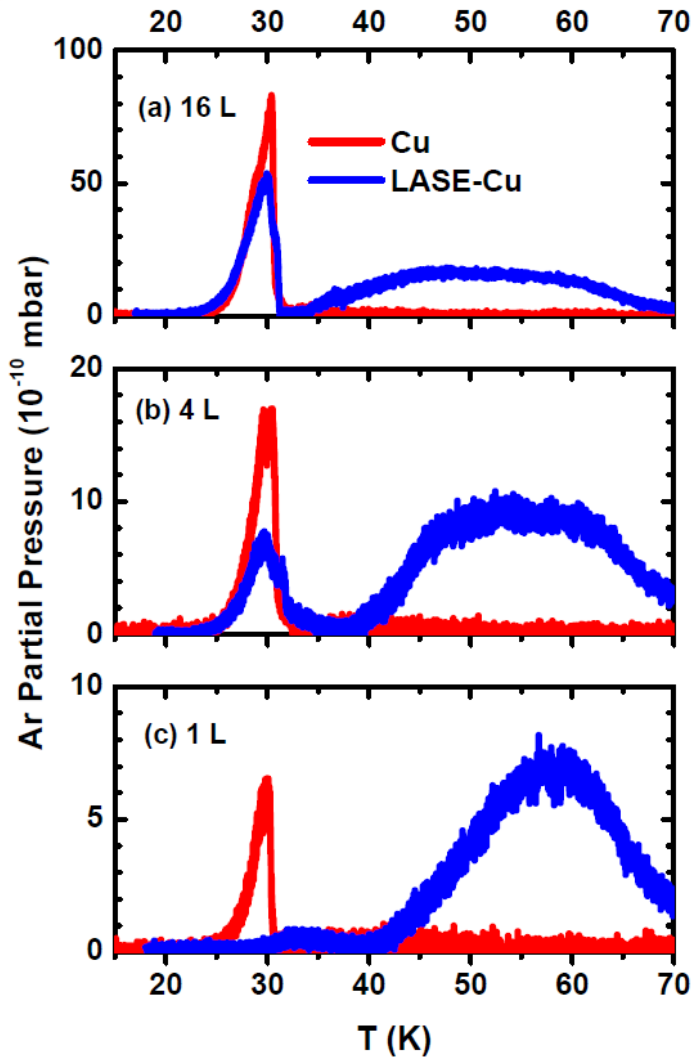
1 L on clean Cu



16 L on clean Cu



At a fixed gas dose, the desorption of Ar on flat substrate is decisive to single out both the sample and the spurious contribution at that dose



➤ On flat Cu Ar adsorbs due to the weak Ar-Cu and Ar-Ar Van der Waals interactions and the desorption curve consists of the sharp peak at $T \sim 30$ K.

➤ For the LASE-Cu substrate the Ar adsorption energy at the undercoordinated surface defect sites increases and desorption occurs at higher T. However, at high coverage, multilayer desorption at $T \sim 30$ K is also observed.

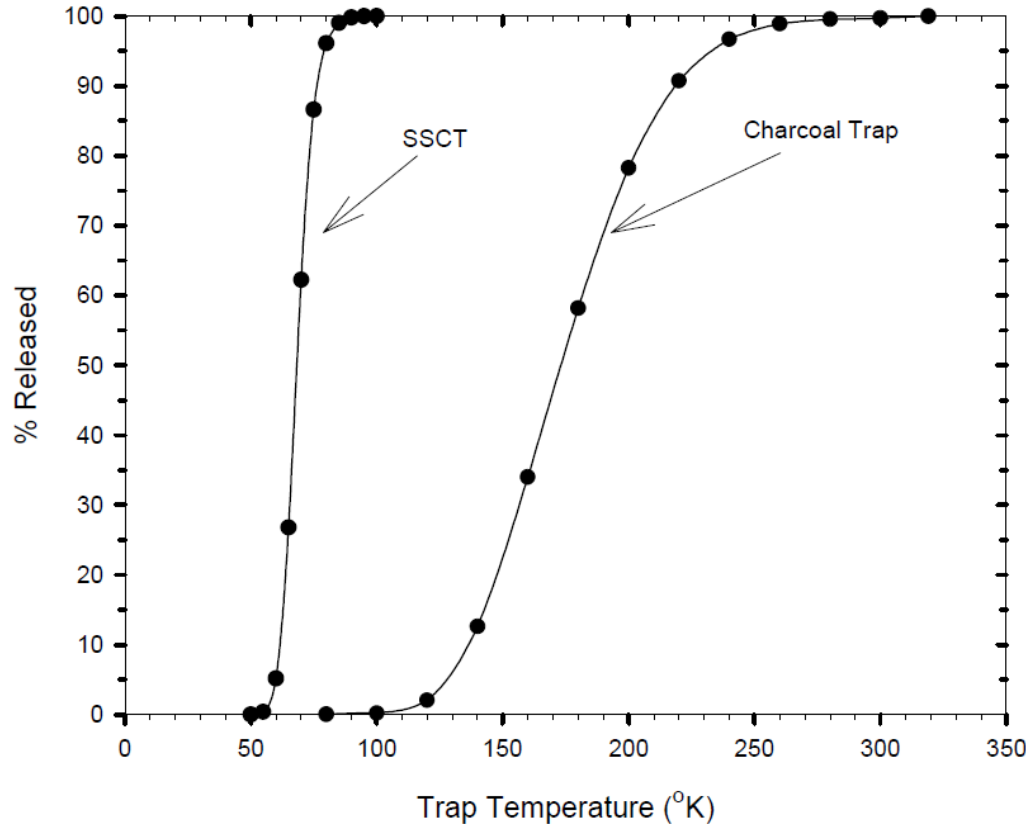


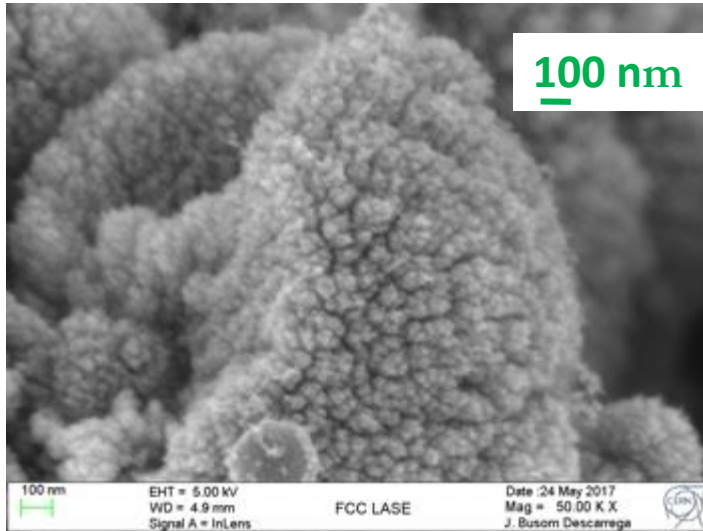
Figure 5. A comparison of the SSCT and charcoal cryogenic trap release characteristics for argon as a function of temperature.

Improvements in noble gas separation methodology: A nude cryogenic trap

Dempsey E. Lott III

Department of Marine Chemistry and Geochemistry, Woods Hole Oceanographic Institution, Woods Hole, Massachusetts 02543, USA (dlott@whoi.edu)

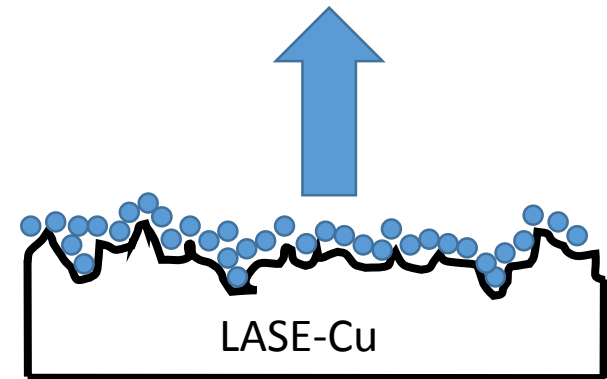
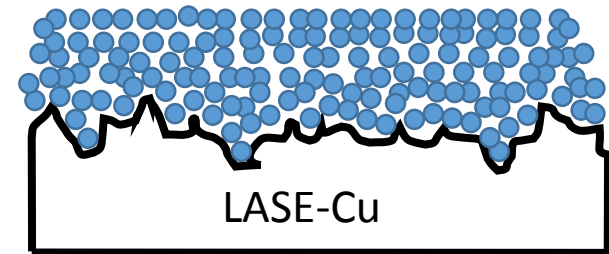
Desorption processes in charcoal and other cryotrap



Morphology of LASE-Cu by SEM

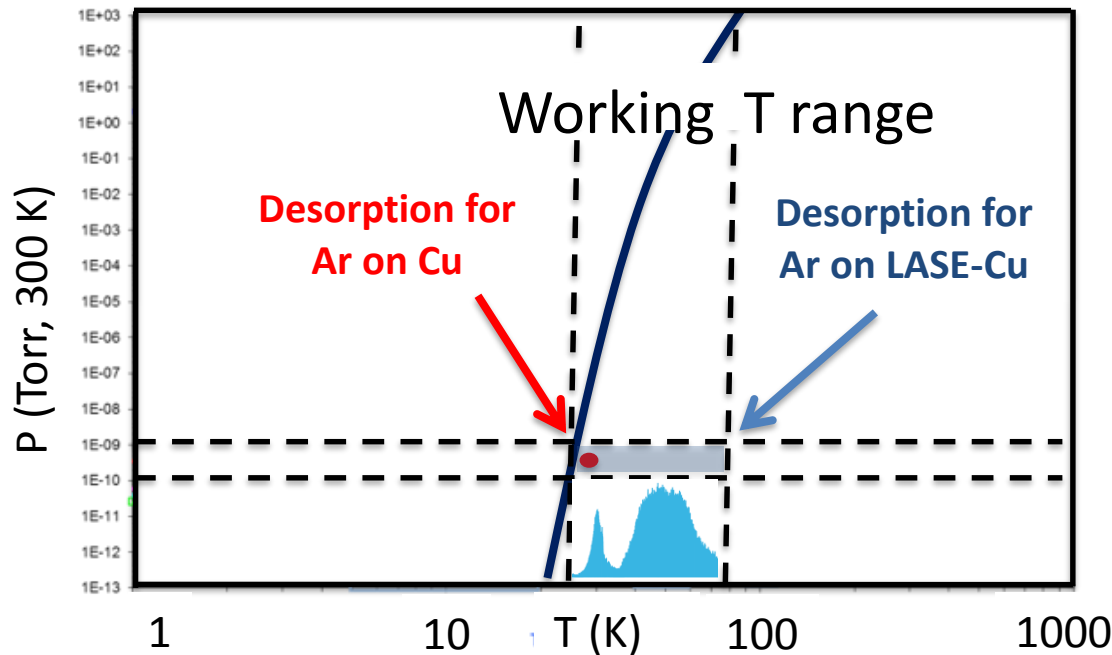
Highly rough and inhomogeneous surface
with nanometric features
(undercoordinated surface defect sites)

At higher coverages the desorption is dominated by usual Ar/Ar Van-der-Waals interaction



At low coverages the desorption is dominated by Ar/LASE interaction

Saturated vapour pressure from Honig and Hook (1960) (C2H6 Thibault et al.)



For ices dominated by Ar-LASE, Ar desorbs both at $T \sim 25-30$ K and in a much wider range

WARNING: If confirmed, the use of highly porous materials at LT must be considered with great care!

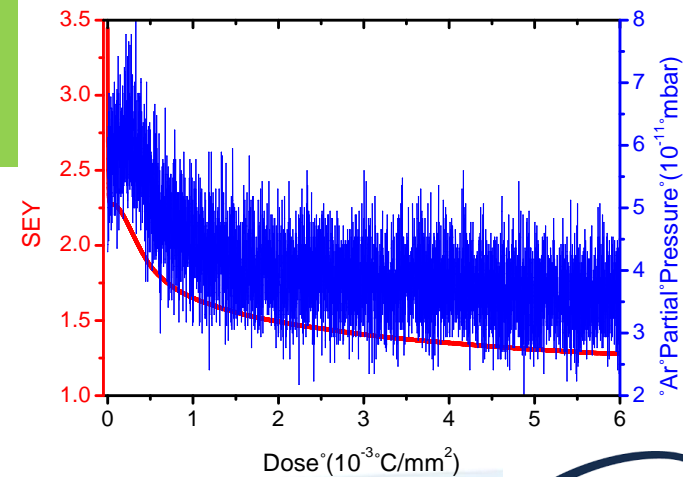
Technical work

- Gas-line assembly
- Assembly and test of the new heater



Outlook

- CO, CO₂, CH₄ desorption studies
- Electron and photo-desorption investigations





The team at LNF

E. La Francesca **R. Cimino** **R. Larciprete**
M. Angelucci **A. Liedl**

DAΦNE-L

